Monte Carlo simulations of a CZT detector for post accidental dosimetry

Anna Selivanova[1, *], Jiří Hůlka[1], Tomáš Vrba[2], and Irena Češpírová[1]

[1]*National Radiation Protection Institute (SURO), Bartoškova 1450/28, Prague, 140 00, Czech Republic*
[2]*Czech Technical University in Prague, Břehová 78/7, Prague, 115 19, Czech Republic*
*Corresponding author's e-mail: anna.selivanova@suro.cz

Abstract. This work is focused on Monte Carlo (MC) simulations of a small CZT detector considering radiation or nuclear accidents. The CZT detectors seem to be convenient for on site/unmanned aerial vehicle measurements in these cases. Therefore, assuming possible emergency scenarios, the MC simulations were performed using the MCNP6.1 transport code. A mathematical model of the detector was based on sketches from the manufacturer and X-ray images. The detector model was validated with a radium (^{226}Ra) needle and a standard ^{60}Co source. Differences between simulations and measurements did not exceed 4 %, therefore we accepted the model. Afterwards, efficiency calibrations for selected industrial and medical sources were prepared, as well as calculations for semi-infinite surface contamination with artificial radionuclides. *In situ* measurement geometry at 1 m above the ground and measurements with drones at chosen heights (> 1 m) were supposed. For MDA values estimation, natural background spectra were simulated respecting specific activities of natural radionuclides in soil in the Czech Republic. Depending on the detector heights and considering acquisition time of 5 s, MDAs were in a range of several MBq to GBq for point sources, while in the case of surface contamination, MDAs were equal to hundreds of kBq m^{-2}.

KEYWORDS: Monte Carlo simulations; CZT detectors; radiation/nuclear accidents.

1 INTRODUCTION

This work is dedicated to continuing Monte Carlo simulations of a CZT detector described in [1] and subsequent field measurements. Owing to a drone renovation and technical limitations, field conditions were simulated in a laboratory. However, UAV (unmanned aerial vehicle) measurements with the same model of the CZT detector were already carried out by P. G. Martin [2]. As well as in the earlier research, the mathematical model of the selected CZT detector was tested in geometries relevant for measurements on site or using drones in emergency situations (e.g. after radiation/nuclear accidents). Two geometries, an orphan source and a large-scale surface contamination, were considered. For an abandoned source geometry, Monte Carlo simulations of small sealed sources with real physical parameters were prepared. Assuming an extensive surface contamination, a quasi-infinite surface planar geometry was tested. Contrary to previously employed simplified source set-ups within Monte Carlo modelling [1], changes of a source effective radius with the detector height were investigated more in details. Simulated efficiencies and simulated/measured background spectra were used for an estimation of minimum detectable activities (MDA). Then a radiation mapping test was carried out.

2 MATERIALS AND METHODS

2.1 The CZT detector

All simulations and measurements were related to the spectrometric CZT detector [3]. Using a mathematical model of the detector [1], Monte Carlo simulations were performed in the MCNP6.1 transport code [4]. To score the detector responses, the F8 tally (pulse-height distribution) was used. The model was validated using a radium needle aligned with the detector entrance window center. The verification also included tests with a ^{60}Co point source located laterally from the detector. Differences between measurements and simulations were ≤ 4 %, then the model was considered to be validated for chosen conditions [1].

2.2 Small sealed sources

To prepare efficiency calibrations for orphan sources, two radionuclides (^{137}Cs and ^{60}Co) with three energies (661.66 keV, or 1173.23 keV and 1332.49 keV) were anticipated, assuming real sealed source geometries (small cylinders). Spatial parameters of both sources are in Table 1. For ^{137}Cs, a material density of an active part (cesium chloride) was set equal to 2.5 g cm^{-3}, according to [5]. In

case of ^{60}Co, an active part density (cobalt) was 8.86 g cm^{-3}. A material of the ^{137}Cs source capsule was the 316L stainless steel, while a capsule of the ^{60}Co source was made from the 321 stainless steel. Densities of both materials were 8.0 g cm^{-3} [6]. Nominal activities of anticipated sources were approximately 2 GBq and 3 GBq for ^{60}Co, resp. ^{137}Cs. Within Monte Carlo modelling, two source positions were tested, a vertical position (with active parts oriented downwards) and a horizontal position. Centers of capsules were aligned with the center of the detector entrance window. Due to expected measurements *in situ* or with drones, seven detector heights above the ground were assumed, 1–30 m [1]. Thereafter, efficiencies of small sealed sources were compared with efficiencies of ideal point sources [1].

Table 1: Dimensions and materials of real sealed sources

Radionuclide	Active part diameter (mm)	Active part height (mm)	External diameter (mm)	External height (mm)	Side wall/bottom thickness (mm)
^{137}Cs	4	4	6	8	1
^{60}Co	3	3	5	10	1

2.3 Surface planar sources

Two selected detector heights (1 m and 10 m) above the ground were tested. Three artificial radionuclides (^{131}I, ^{137}Cs and ^{134}Cs) with four energies (364.49 keV, 661.66 keV, 604.72 keV and 795.86 keV) were simulated. Soil composition and its density (1.52 g cm^{-3}) was set according to the material *Earth, U. S. Average* [6]. Considering artificial radionuclides freshly deposited on soil surfaces, a terrain roughness was taken into account again, setting a relaxation depth to 1 mm [7]. The preceding research employed a simplified approach to set-up a source radius large enough to resemble an infinite surface planar source [1]. A constant ratio between the surface planar source radius and the detector height equal to 150 was used. The approximation was based on the test with ^{137}Cs only and the height of 1 m above the ground. However, control simulations for ^{137}Cs and the detector at 10 m demonstrated that the applied approach was very conservative. Therefore, in order to estimate parameters of quasi-infinite surface planar sources more precisely, changes of the effective source radius at two detector heights were investigated. All sets for heights of 1 m and 10 m consisted of simulations with increasing source radii, where maximum radius values were equal at least to a product of heights and a factor of 150. Simulated efficiencies were renormalized to source areas and emission yields. Obtained responses were in counts s^{-1} Bq^{-1} m^{2}. Thereafter, the detector responses were followed in relation to sources with the largest radius.

2.4 Background spectra

Simulations of background spectra have already been described in [1]. Simulated spectra corresponded to specific activities of ^{40}K (1409 Bq kg^{-1}), ^{232}Th (190 Bq kg^{-1}), ^{238}U/^{226}Ra (211 Bq kg^{-1}). To compare simulations with measurements, one background spectrum was acquired. Due to the subsequent radiation mapping test, the spectrum acquisition was carried out in the same laboratory. The detector was fixed at 1 m above a floor. A live time of the measurement was set to 20 minutes as a possible drone operation time.

2.5 MDA determination

2.5.1 MDAs for 1 m

All MDA values were assessed using the Currie's formula [8]. Considering the detector at 1 m above the ground and a sample acquisition time of 5 s, MDAs were calculated for ideal point sources (^{137}Cs and ^{60}Co) using the real background spectrum. In order to consider a usability of the simulated background spectrum for rough orientational MDA assessments, MDAs from measurements were compared with MDAs based on simulations [1]. Calculated MDA values were used within preparations of the field test, where a standard point source (small drop on filters in polymethyl methacrylate capsules) was used.

2.5.2 Height dependence

Expecting measurements with drones, MDAs of small sealed and surface planar sources for selected heights of the detector above the ground were calculated. An acquisition time of 5 s was assumed. Simulated background spectra were adopted from the earlier work [1]. For the detector at 1 m above the ground and an infinite surface contamination, the source radius of 200 m was anticipated. Considering the detector at 10 m, the surface planar source radius equal to 300 m was chosen. In cases of several energies of one radionuclide, the lowest MDA was chosen. Afterwards, all obtained MDA values were compared with previous results [1].

2.6 Field measurements

To test the CZT detector in real conditions, the radiation mapping test with ^{137}Cs was prepared in the laboratory. An auxiliary grid was drawn on floor tiles. An area of one floor tile was 900 cm^2 (30 cm × 30 cm). The mapped area was 480 cm × 360 cm. The detector was at 1 m above the floor with the entrance window oriented downwards. All measurement points were located in centers of floor tiles. Distances between two points were 60 cm in both axes (*x* and *y* axis). Acquisition times of 5 s was selected. To set the source activity above the MDA, standard point sources were fixed together with an adhesive tape, in accordance with [1] and paragraph 2.5.1. The summary activity on the day of measurements was equal to 3.52 MBq. Then, a map of total counts rates and count rates in a region of interest (ROI) was created.

3 RESULTS

3.1 Small sealed sources

Simulated efficiencies for real sources in vertical positions with active parts oriented downwards and in horizontal positions are in Table 2. Statistical uncertainties of efficiencies were ≤ 0.1 %. Table 3 summarizes ratios of simulated efficiencies for real sources in both positions and efficiencies for ideal point sources adopted from [1].

Table 2: Simulated efficiencies ε for real sealed sources in vertical/horizontal position

Vertical position								
Height (m)		1	2	3	5	10	20	30
Nuclide	Energy (keV)	ε	ε	ε	ε	ε	ε	ε
^{137}Cs	661.66	3.99E-07	9.95E-08	4.39E-08	1.56E-08	3.72E-09	8.47E-10	3.43E-10
^{60}Co	1173.24	1.31E-07	3.29E-08	1.46E-08	5.18E-09	1.25E-09	2.92E-10	1.21E-10
^{60}Co	1332.50	1.09E-07	2.72E-08	1.20E-08	4.29E-09	1.04E-09	2.44E-10	1.01E-10
Horizontal position								
^{137}Cs	661.66	4.47E-07	1.12E-07	4.92E-08	1.74E-08	4.17E-09	9.50E-10	3.85E-10
^{60}Co	1173.24	1.65E-07	4.12E-08	1.82E-08	6.49E-09	1.57E-09	3.66E-10	1.52E-10
^{60}Co	1332.50	1.34E-07	3.36E-08	1.49E-08	5.30E-09	1.29E-09	3.01E-10	1.25E-10

Table 3: Ratio of simulated efficiencies for sealed sources ε_{real} in vertical or horizontal position and ideal point sources ε_{point}

Vertical position								
Height (m)		1	2	3	5	10	20	30
Nuclide	Energy (keV)	$\varepsilon_{real}/\varepsilon_{point}$	$\varepsilon_{real}/\varepsilon_{point}$	$\varepsilon_{real}/\varepsilon_{point}$	$\varepsilon_{real}/\varepsilon_{point}$	$\varepsilon_{real}/\varepsilon_{point}$	$\varepsilon_{real}/\varepsilon_{point}$	$\varepsilon_{real}/\varepsilon_{point}$
^{137}Cs	661.66	0.81	0.81	0.81	0.82	0.82	0.82	0.83
^{60}Co	1173.24	0.72	0.71	0.72	0.73	0.72	0.72	0.73
^{60}Co	1332.50	0.73	0.73	0.73	0.75	0.74	0.74	0.74
Horizontal position								
^{137}Cs	661.66	0.91	0.91	0.91	0.92	0.92	0.92	0.93
^{60}Co	1173.24	0.90	0.90	0.90	0.92	0.90	0.91	0.91
^{60}Co	1332.50	0.91	0.90	0.90	0.92	0.91	0.91	0.91

3.2 Surface planar sources

Efficiencies for surface planar sources and the detector at 1 m and 10 m are in Table 4. Statistical uncertainties of all simulated efficiencies were ≤ 0.5 %. Corresponding response ratios are in Table 5.

Table 4: Simulated efficiencies ε for surface planar sources with varied radii

Detector height of 1 m above the ground								
Radionuclide	^{131}I		^{134}Cs				^{137}Cs	
Energy (keV)	364.49		604.72		795.86		661.66	
Radius (m)	ε	Response	ε	Response	ε	Response	ε	Response
10	6.22E-08	1.59E-05	2.40E-08	7.35E-06	1.48E-08	3.98E-06	2.04E-08	5.44E-06
100	9.25E-10	2.36E-05	3.70E-10	1.14E-05	2.34E-10	6.27E-06	3.17E-10	8.47E-06
150	4.15E-10	2.38E-05	1.67E-10	1.15E-05	1.06E-10	6.39E-06	1.43E-10	8.61E-06
200	2.34E-10	2.39E-05	9.44E-11	1.16E-05	5.99E-11	6.43E-06	8.11E-11	8.67E-06
300	1.04E-10	2.39E-05	4.22E-11	1.16E-05	2.68E-11	6.48E-06	3.60E-11	8.65E-06
Detector height of 10 m above the ground								
50	1.40E-09	8.92E-06	5.61E-10	4.30E-06	3.55E-10	2.38E-06	4.81E-10	3.21E-06
100	4.24E-10	1.08E-05	1.74E-10	5.33E-06	1.11E-10	2.98E-06	1.50E-10	3.99E-06
200	1.13E-10	1.15E-05	4.73E-11	5.80E-06	3.06E-11	3.29E-06	4.09E-11	4.37E-06
300	5.06E-11	1.16E-05	2.14E-11	5.90E-06	1.39E-11	3.36E-06	1.85E-11	4.44E-06
1500	2.03E-12	1.16E-05	8.58E-13	5.92E-06	5.59E-13	3.38E-06	7.43E-13	4.46E-06

Table 5: Detector response ratios for surface planar sources with varied source radii

Detector height of 1 m above the ground				
Radionuclide	^{131}I	^{134}Cs		^{137}Cs
Energy (keV)	364.49	604.72	795.86	661.66
Radius (m)	Response ratio to @300 m			
10	0.66	0.63	0.61	0.63
100	0.99	0.98	0.97	0.98
150	1.00	0.99	0.99	1.00
200	1.00	1.00	0.99	1.00
300	1.00	1.00	1.00	1.00
Detector height of 10 m above the ground				
Radius (m)	Response ratio to @1500 m			
50	0.77	0.73	0.70	0.72
100	0.93	0.90	0.88	0.90
250	1.00	0.99	0.99	0.99
300	1.00	1.00	0.99	1.00
1500	1.00	1.00	1.00	1.00

3.3 MDA determination

3.3.1 MDAs for 1 m

MDAs for ideal point sources calculated using both the real background spectrum and Monte Carlo simulations for the detector at 1 m and the acquisition times of 5 s are listed in Table 6.

Table 6: MDA values for ideal point sources for the detector at 1 m (acquisition time of 5 s)

Background spectrum		Measurement – 20 min	Monte Carlo simulation
Nuclide	Energy (keV)	MDA (MBq)	MDA (MBq)
^{137}Cs	661.66	3.35	3.26
^{60}Co	1173.24	6.21	6.25
^{60}Co	1332.50	5.52	6.52

3.3.2 Height dependence

MDAs of sealed sources in both chosen positions are summarized in Table 7. MDA dependences on the detector height for both sources positions are shown in Fig. 1. MDA values for surface planar sources are in Table 8, as well as MDAs from the previous research [1].

Figure 1: MDA values depending on the detector height for small sealed sources both in vertical and horizontal position (acquisition time of 5 s)

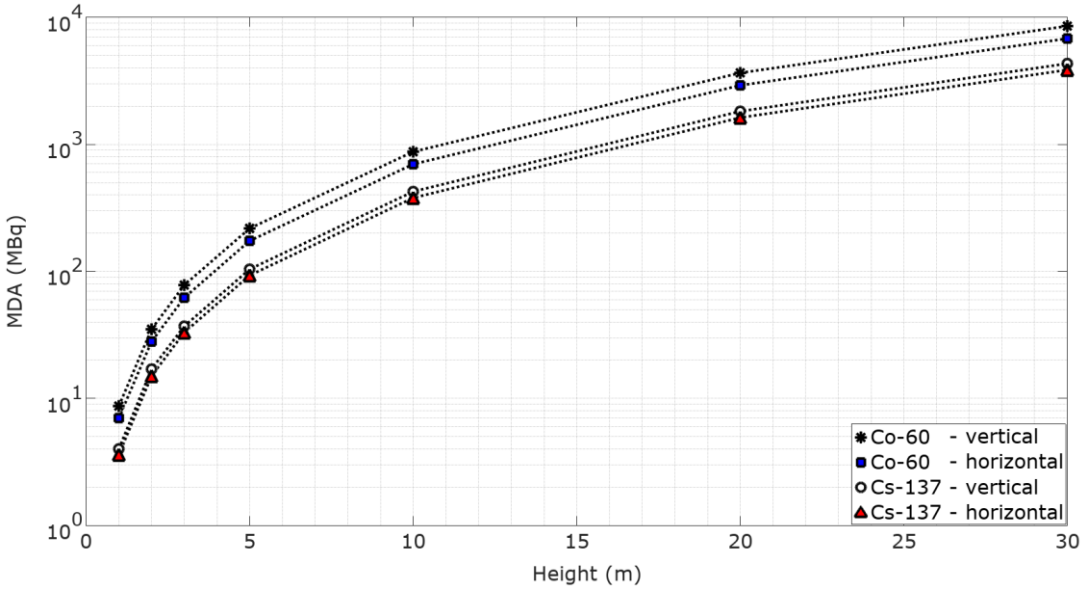

Table 7: MDA values for sealed sources in vertical and horizontal position (acquisition time of 5 s)

Vertical position							
Height (m)	1	2	3	5	10	20	30
Nuclide	MDA (MBq)	MDA (MBq)	MDA (MBq)	MDA (MBq)	MDA (MBq)	MDA (MBq)	MDA (MBq)
^{137}Cs	4.0	17	37	104	425	1821	4329
^{60}Co	8.7	35	78	218	875	3654	8538
Horizontal position							
Height (m)	1	2	3	5	10	20	30
Nuclide	MDA (MBq)	MDA (MBq)	MDA (MBq)	MDA (MBq)	MDA (MBq)	MDA (MBq)	MDA (MBq)
^{137}Cs	3.6	15	33	93	379	1624	3861
^{60}Co	7.0	28	62	174	698	2915	6812

Table 8: MDA values for quasi-infinite surface planar sources (acquisition time of 5 s)

Nuclide	MDA (kBq m^{-2})	MDA (kBq m^{-2})	MDA (kBq m^{-2})	MDA (kBq m^{-2})
^{131}I	91	180	92	179
^{137}Cs	157	302	158	301
^{134}Cs	178	335	179	333
Height (m)	1	10	1	10
Radius (m)	200	300	150	1500

3.4 Field measurements

Maps of count rates (whole spectra and ROI) from the test with ^{137}Cs are in Fig. 2. Actual source positions were depicted as small asterisks.

Figure 2: Count rates maps for measurements with ^{137}Cs

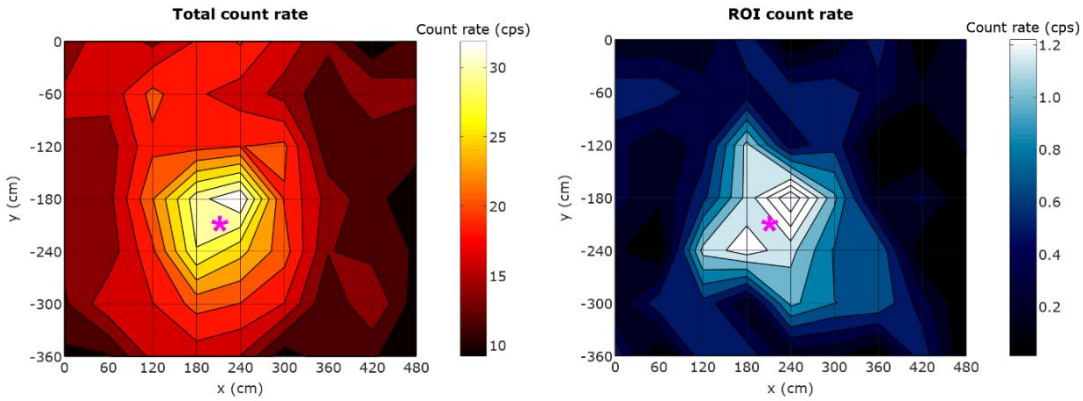

4 DISCUSSION

4.1 Small sealed sources

From the simulation results in Table 2, all efficiency values for sealed sources were lower than ideal point source efficiencies [1]. According to the IAEA Technical Document #1690 [9], materials of source constructions partially absorb own source radiation, therefore obtained results agreed with the mentioned publication. Higher efficiency values for small sealed sources corresponded to sources located horizontally. Comparing with efficiencies for point sources, differences were in a range of 7–10 % (Table 3). In the horizontal position, active parts were shielded with 1 mm of 316L steel or 321 steel for ^{137}Cs, resp. ^{60}Co (Table 1). Lower efficiency values were observed for sources placed vertically, differed by 17–29 % in comparison with ideal point sources (Table 3). For this source position, shielding layers were 3 mm of 316L steel for ^{137}Cs and 6 mm of 321 steel for ^{60}Co (Table 1). Thereafter, both construction materials and source positions due to radiation self-absorption affected efficiency values. Nevertheless, source constructions could vary or point-like unshielded standard sources could be even hidden inside layers of different densities, e.g. in scrap yards. Hence, the use of efficiencies for ideal point sources could underestimate real activities up to several tens of percent and require taking into consideration of real conditions.

4.2 Surface planar sources

According to Table 4, for the detector at 1 m, a saturation of responses started roughly at the source radius of 150–200 m. This interval corresponded to the response losses ≤ 1 % (Table 5). Therefore, for subsequent MDA calculations of all anticipated radionuclides and the detector at 1 m, efficiencies for sources with the more conservative radius of 200 m were chosen instead of previously used 150 m [1]. Supposing the detector at 10 m, the response plateau corresponded to an interval of the source radius of 250–300 m (Table 4). Considering the source radius of 300 m, losses of responses did not exceed 1 % (Table 5) and were neglected, as well as for the height of 1 m. Thereafter, for the height of 10 m above the ground, effective radii of all sources were set to 300 m instead of 1500 m used before [1]. In accordance with J. D Allyson [10], for a NaI(Tl) detector in higher positions (50–125 m), responses saturated roughly at 300–500 m of the source radius. Afterwards, the earlier employed simplified maintenance of a constant field of view based on simulations with ^{137}Cs corresponded with results presented in the current paper, as well as generally with J. D Allyson [10].

4.3 MDA determination

4.3.1 MDAs for 1 m

In accordance with Table 6, in case of the detector at 1 m and the acquisition time of 5 s, MDAs for ideal point sources of ^{137}Cs and ^{60}Co were equal to several MBq. These activities could correspond to calibration/check sources [11]. Anticipating ^{137}Cs and the acquisition time of 5 s, MDA values from

simulations were slightly lower than from the measurement. The difference between both values (3.26 MBq, resp. 3.35 MBq) equal to 3 % possibly originated in the presence of ^{137}Cs in the laboratory. Nevertheless, the discrepancy between the simulation and the measurement for ^{137}Cs was not strong and could be neglected within orientational MDA estimations for the laboratory conditions. In case of ^{60}Co and 1173.24 keV, simulated MDAs were almost the same as values from measurements. For 1173.24 keV, both MDA values were approximately 6.2 MBq, with the difference < 1 %. However, for 1332.50 keV, the MDA from simulations (6.52 MBq) was higher by 18 % than the value from the measurement (5.52 MBq). The difference originated from a lower contribution to measured spectra in this energy region (less counts) contrary to simulations. Nevertheless, the more conservative MDA value would allow to choose better measurement set-ups in case of lost/abandoned sources with a known/expected activity. Thereafter, the conservatively simulated spectrum of natural background could be used for rough MDA estimations of one radionuclide, e.g. within preliminary measurement preparations, anticipating a normal natural background.

4.3.2 Height dependence for sealed sources

From the results in Table 7, MDA values for small sealed sources in both positions were in a range of several MBq to GBq. Hence, supposing the detector heights of 1–30 m above the ground and the sampling time of 5 s, standard calibration sources or sources for medical/industrial purposes could be detected [11]. According to Fig. 1, MDAs of small sealed sources depended on source orientations. For the vertical position (with active parts in capsule bottoms), MDA values were higher contrary to sources located horizontally. The dissimilarities in MDA values were caused by sources constructions and shielding with steel of different thicknesses (paragraph 4.1). In case of MDAs for ^{137}Cs, differences between vertical and horizontal positions were 12 %, while for ^{60}Co MDAs differed by 25 %. Comparing MDA values for small sealed sources and ideal point sources [1], MDAs of ideal point sources were slightly lower. Considering sealed sources in the vertical position, ideal point source MDAs differed by 16–28 %. For small sources placed horizontally, the difference was in a range of 5–10 %. Both MDA underestimations for point sources roughly corresponded to discrepancies in efficiency values (paragraph 4.1). Assuming the acquisition time of 5 s, the small sealed ^{137}Cs source with the expected activity of 3 GBq could be detected roughly up to 20 m within UAV measurements, for both orientations (Table 7). In case of the sealed ^{60}Co 2 GBq source, the detector would detect the source in both positions up to 10–20 m (Table 7). However, according to graphs for sealed sources in Fig. 1, the ^{137}Cs source with 3 GBq would be most probably revealed roughly up to 25 m, while for ^{60}Co and 2 GBq the maximum MDA height would be about 15 m above the ground. Afterwards, although MDAs were influenced by source constructions and positions, orientational heights of the detector were similar, regardless geometries of sources (Table 7). Moreover, very similar MDAs for ideal point sources [1] could be employed for either rough assessments within mission planning for emergencies with small sources, or for known point-like standard sources.

4.3.3 Height dependence for surface planar sources

According to Table 8, MDAs for quasi-infinite surface planar sources were in a range of hundreds of kBq m^{-2}, both for the detector at 1 m and 10 m above the ground. Comparing MDA values for sources with conservative radii [1], all MDAs were almost the same, with practically negligible differences of 1–2 kBq m^{-2} (or ≤ 1 %). Therefore, in order to simplify simulations, the effective source radius could be used within modelling of quasi-infinite surface planar sources.

4.4 Field measurements

The total activity on the day of measurements of the ^{137}Cs point source was slightly above the MDA for the laboratory conditions (paragraph 4.3.1). Based on count rate maps for ^{137}Cs (Fig. 2), spots with higher cps indicated possible locations of the radioactive source. The source could be revealed both from total count rates in whole spectra and from count rates in ROIs. For the map of total count rates, the maximum count rate corresponded to the point 42 cm roughly distant (half of hypotenuse) from the

actual source position. In case of the map of ROI count rates, two spots could be seen, while the left hot spot was actually accidental. Observed discrepancies in both maps were possibly caused by the low ^{137}Cs activity (only 5 % above the MDA) and the shorter acquisition time (5 s). Nevertheless, within the radiation mapping with the selected set-up of the CZT detector, the presence of the ^{137}Cs source with the activity > MDA was recognized, as well as the orientational source position. Afterwards, the CZT detector and the tested measurement set-up seemed to be proper for the radiation mapping and searching for orphan sources.

5 CONCLUSION

Results of Monte Carlo simulations with the CZT detector demonstrated that constructions of sealed sources and their orientations had an impact on efficiency values. Therefore, the use of efficiencies for ideal point sources could underestimate activities of sealed sources up to tens of percent. In case of surface planar sources, the effective source radius changed with the height, while the response saturation approximately resembled the published data. Comparing MDA values from the simulated and measured background spectrum, simulated values were both almost the same or higher than measurements. Therefore, the simulated spectrum could be used for rough MDA estimations within measurement preparations. For the detector heights of 1–30 m and the acquisition time of 5 s, MDAs for sealed sources were in a range of several MBq to GBq, being very similar to values for ideal point sources. For quasi-infinite surface planar sources and the use of sources with effective radii instead of conservative parameters, obtained MDAs were hundreds of kBq m^{-2}, as well as in the previous work. Based on the simulated MDAs, the radiation mapping test was carried out. Using the selected set-up, the test clearly revealed the ^{137}Cs point source with the activity slightly above the MDA.

6 REFERENCES

[1] A. Selivanova, J. Hůlka, T. Vrba, and I. Češpírová, "Efficiency calibration of a CZT detector and MDA determination for post accidental unmanned aerial vehicle dosimetry," *Appl. Radiat. Isot.*, vol. 154, 2019.

[2] P. G. Martin, O. D. Payton, J. S. Fardoulis, D. A. Richards, Y. Yamashiki, and T. B. Scott, "Low altitude unmanned aerial vehicle for characterising remediation effectiveness following the FDNPP accident," *J. Environ. Radioact.*, vol. 151, pp. 58–63, Jan. 2016.

[3] Kromek Group PLC, "GR1 CZT gamma-ray detector spectrometer," 2020. [Online]. Available: https://www.kromek.com/product/gamma-ray-detector-spectrometers-czt-based-gr-range/. [Accessed: 02-Mar-2020].

[4] T. Goorley *et al.*, "Initial MCNP6 release overview," *Nuclear Technology*. 2012.

[5] E. Lamb, "Cesium-137 Source Material for An Irradiator. No. CONF-800964-1.," Oak Ridge National Lab., Oak Ridge, Tennessee, 1980.

[6] R. J. McConn Jr, C. J. Gesh, R. T. Pagh, R. A. Rucker, and R. G. Williams III, "Compendium of Material Composition Data for Radiation Transport Modeling - Revision 1, PIET-43741-TM963, PNNL-15870 Rev. 1," 2011.

[7] UNSCEAR, *Sources and Effects of Ionizing Radiation. Official Records of the General Assembly UNSCEAR 2000 Report to the General Assembly, with Scientific Annexes. ANNEX A – Dose Assessment Methodologies.*, vol. I. New York: United Nations, 2000.

[8] L. A. Currie, "Limits for qualitative detection and quantitative determination. Application to radiochemistry," *Anal. Chem.*, vol. 40, no. 3, pp. 586–593, Mar. 1968.

[9] IAEA, *Review of Sealed Source Designs and Manufacturing Techniques Affecting Disused Source Management. IAEA-TECDOC-1690*. Vienna: International Atomic Energy Agency, 2012.

[10] J. D. Allyson, "Environmental Gamma-Ray Spectrometry: Simulation of Absolute Calibration of In-Situ and Airborne Spectrometers for Natural and Anthropogenic Sources," University of Glasgow, 1994.

[11] H. Domenech, *Radiation safety: Management and programs*, 1st ed. Cham, Switzerland: Springer International Publishing, 2016.